DOI: 10.1002/ejoc.200600966

Modular P-Chirogenic Aminophosphane-Phosphinite Ligands for Rh-Catalyzed Asymmetric Hydrogenation: A New Model for Prediction of Enantioselectivity

Christophe Darcel,*[a] Dominique Moulin,[b] Jean-Christophe Henry,[c] Michaël Lagrelette,[a] Philippe Richard,[a] Pierre D. Harvey,[d] and Sylvain Jugé*[a]

Keywords: Rhodium / P ligands / Aminophosphane-phosphinites / Hydrogenation / Asymmetric catalysis

An original series of P-chirogenic aminophosphane-phosphinite (AMPP) ligands has been synthesized from (+)- or (–)-ephedrine in 23 to 61 % overall yields by a versatile three-step methodology. The AMPP ligands, bearing either one or two P-chirogenic centers, were used in the form of rhodium complexes for the catalyzed hydrogenation of α-acetamidocinnamate as a test reaction. Notably, even with AMPP ligands all derived from (+)-ephedrine, variation of the substituent on a P-center allowed the phenylalanine derivatives to be obtained in either (*S*) or (*R*) absolute configurations, with *ee* values ranging from 99 % (*S*) to 88 % (*R*). The asymmetric induction was analyzed with the aid of X-ray structures of AMPP complexes, and a new model for the enantioselectivity, taking into consideration the boat conformation and the steric and electronic dissymmetries at the dihydride rhodium-substrate complex, has been proposed. This model offers an alternative to the quadrant rule, well adapted to the C_2-symmetry ligands and the chair conformation of their complex derivatives. In this work, the model, which schematizes the front side of the complex as a sextant in the direction of the cardinal points, fits with coordination of the substrate by the acetamido and the cinnamyl groups in the north and east (or west) parts, respectively. The enantioselectivity originates from the ligand residues located at the south-east or south-west parts of the dihydride rhodium intermediate. Computer modeling on several AMPP-rhodium complexes with PCModel confirms the proposed predicting model.

Introduction

Chiral transition metal complexes have given considerable impetus to asymmetric catalysis, which is today one of the most efficient methods for the synthesis of enantiomerically enriched compounds.[1] Indeed, several reactions involving carbon–hydrogen,[2–6] carbon–carbon,[7–10] or carbon–heteroatom[11–15] bond formation provide highly asymmetric induction for various substrates, and some of them are applied on industrial scales for the production of substances with useful agrochemical, flavor, or pharmaceutical properties.[2,3,6] To improve an asymmetric catalytic reaction for a new substrate is not trivial, however, possible approaches being mainly restricted either by the availability of a library of chiral ligands,[3,6] or to the easy structure modification of an efficient lead series such as BINAP,[16,17] DUPHOS,[18] PHOX,[19] monophos,[20] etc. In particular, the phosphorus and phosphinous derivatives usually prepared by treatment of PCl_3 or chlorophosphanes with available chiral diols,[21,22] binaphthol,[23–25] or amino alcohols[26–31] offer an efficient and easy route to new chiral ligands. Notably, the phosphorus ligands are by far the most commonly used ones,[16-31] because they offer far more possibilities for modification of the structure (mono-, di-, multidendate, hemilabile, hybrids, etc.), the symmetry (C_2, dissymmetric, etc.), the basicity, and the chirality at the phosphorus atom.

Prediction of the enantioselectivity of the hydrogenation – catalyzed by rhodium complexes – of a substrate such as **1** has previously been possible with the aid of the quadrant diagram rule[32,33] initially proposed by Knowles, but recently reformulated by other research groups using numerous other C_2-symmetry ligands.[33,34] The quadrant diagram describes the chiral environment of the rhodium atom as four areas, in order to take account of the relative bulkiness of the ligand substituents, which may be placed at axial or equatorial positions as a result of the twisted-chair con-

[a] Laboratoire de Synthèse et d'Électrosynthèse Organométalliques (LSEO), UMR CNRS 5188, Université de Bourgogne, 9 Avenue A. Savary, BP 47870, 21078 Dijon, France
Fax: +33-3-80396113
E-mail: Christophe.Darcel@u-bourgogne.fr
Sylvain.Juge@u-bourgogne.fr
[b] BASF-Aktiengesellschaft, GCI/B-M 311, 67056 Ludwigshafen, Germany
Fax: +49-621-6059144
E-mail: dominique.moulin@basf-ag.de
[c] SYNTHELOR SAS, 102 impasse H. Becquerel, Dynapôle de Ludres-Fléville, 54510 Ludres, France
Fax: +33-3-83156735
E-mail: jc.henry@synthelor.com
[d] Département de Chimie de l'Université de Sherbrooke, Sherbrooke J1K2R1 Québec, Canada,
Fax: +819-821-8017
E-mail: Pierre.Harvey@USherbrooke.ca

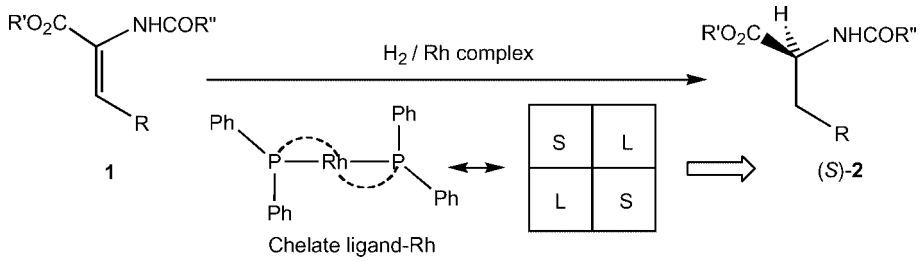

Scheme 1.

formation in the complex (Scheme 1). It is therefore possible to predict the absolute configuration of the hydrogenated product **2**[34] from the relative bulks of the substituents at the corners (Scheme 1).

While the quadrant rule helps to explain the enantioselectivity, prediction of the architecture of the rhodium complex and its stereocontrol in the catalytic hydrogenation of a given substrate is currently still highly speculative. Naturally, much work has been focused on the origin of the enantioselectivity of such reactions, and for a long time it was considered that the selectivity does not stem from the relative stabilities of the substrate–rhodium complexes, but from their rate constants for the oxidative addition of dihydrogen (unsaturated route).[36–44] However, recent experimental and computational data have provided support for a second reaction pathway involving a fast equilibrium of the dihydride–substrate complexes **3**, followed by the stereodetermining migration insertion step[35,45–52] (Scheme 2). Finally, the stereoselectivities of the unsaturated and the dihydride pathways are related, even though in the first, substrate coordination occurs before the oxidative addition of dihydrogen, and in the second, substrate coordination occurs after dihydrogen addition.

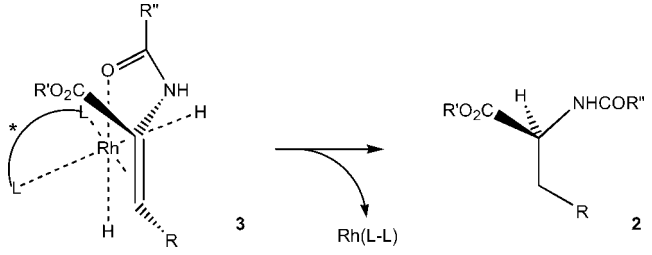

Scheme 2.

From a mechanistic point of view, P-chirogenic ligands have attracted much interest for understanding of the interactions occurring between the prochiral substrate and the catalyst, thanks to the potential offered by the presence of different substituents on the phosphorus atoms. Thus, the P-chirogenic center allows a more sterically and electronically defined architecture about the metal center. As the dihydride substrate complex **3** also possesses a source of chirality at the metal center, it is thus interesting to investigate whether the diastereoselectivity observed at this step can be explained in terms of host–guest interactions (guest = hydrogen or substrate), in order to correlate the ligand with the enantioselectivity. Mechanistic aspects of catalyzed hydrogenation have previously mainly been studied with P-chirogenic C_2 symmetry diphosphanes,[33,47–54] with a few examples of dissymmetric ligands having been mentioned.[55]

Recently, Vogt's team and our own group have independently described a series of modified P-chirogenic EPHOS ligands **4** (Scheme 3) for catalytic asymmetric hydrogenation and hydroformylation reactions involving rhodium complexes.[56–58] These ligands, preparable from ephedrine as starting material by a versatile methodology, offer the potential for modification of the substituents on one or two P-centers. We now wish to report novel modified P-chirogenic EPHOS ligands **4**, together with their use in rhodium-catalyzed hydrogenations of methyl α-acetamidocinnamate **1** (R = Ph; R′,R′′ = Me) as a test reaction. Although the ligands all originate from the same (+)-ephedrine backbone, here we demonstrate for the first time that it is possible to obtain the hydrogenated product **2** in either the (*R*) or the (*S*) configuration with excellent *ee* values, simply by changing the substituent on a P-center. The asymmetric inductions have been analyzed with the aid of X-ray data for related AMPP **4** complexes, allowing us to propose a new prediction model for the enantioselectivity, based on variation of the P-substituents.

Results and Discussion

The modified EPHOS ligands (AMPP) **4** were prepared from the oxazaphospholidine borane **5** (Scheme 3), which was itself obtained in a one-pot reaction from (+)-ephedrine.[59] Compound **5** was treated with organolithium reagents to induce ring-opening reactions to afford products **6**. These were subsequently trapped in situ with achiral chlorophosphanes $R^2{}_2PCl$, and then with borane, to provide the AMPP diborane complexes **7a**–**l** in 30 to 79% yields (Scheme 3, a). This methodology allows the introduction of various R^1 substituents – such as alkyl, cycloalkyl, aryl, or ferrocenyl – onto the aminophosphane residue (Table 1, Entries 1–12). The AMPP diborane complexes **7** are easily purified and stored, while their decomplexation can be accomplished by heating them in toluene at 50–60 °C in the presence of DABCO, to afford the corresponding diastereomerically pure AMPP ligands **4a**–**l** with retention of configuration on the chiral phosphorus atom (Table 1). The free AMPP **4a**–**l** ligands were readily purified by filtration through neutral alumina, and their diastereomeric purities were checked by ^{31}P NMR spectroscopy.

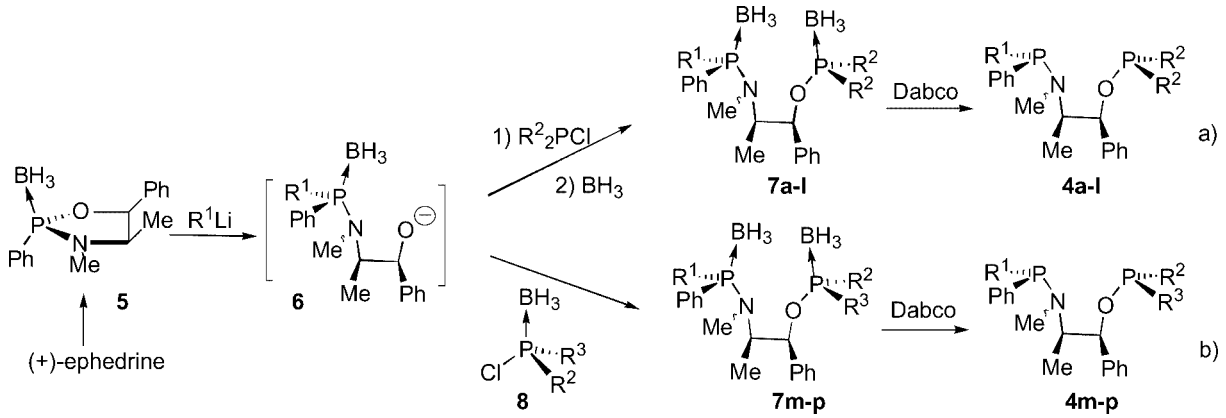

Scheme 3.

Table 1. P-chirogenic aminophosphane-phosphinites (AMPP) **4** and their diborane complexes **7**, synthesized from either (+)- or (–)-ephedrine.

Entry	Ephedrine		R^1	R^2	R^3	AMPP $(BH_3)_2$ **7** yield[a] (%)	AMPP **4** (or **4′**) yield[b] (%)
1	(+)	**a**	Ph	Ph	Ph	63	89
2	(+)	**b**	*o*-An	Ph	Ph	62	91
3	(+)	**c**	*o*-MEMPh	Ph	Ph	66	88
4	(+)	**d**	1-Np	Ph	Ph	62	86
5	(+)	**e**	Fc	Ph	Ph	62	99
6	(+)	**f**	2-Np	Ph	Ph	78	93
7	(+)	**g**	*o*-biPh	Ph	Ph	40	97
8	(+)	**h**	*t*-Bu	Ph	Ph	64	88
9	(+)	**i**	Me	Ph	Ph	79	42
10	(+)	**j**	C_6H_{11}	Ph	Ph	38	97
11	(+)	**k**	*o*-An	C_6H_{11}	C_6H_{11}	67	– [d]
12	(+)	**l**	*o*-An	OPh	OPh	30	90
13	(+)	**m**	Me	Ph	Me	18[c]	– [d]
14	(+)	**n**	Ph	Ph	*o*-An	55	94
15	(+)	**o**	Ph	*o*-An	Ph	55	99
16	(+)	**p**	*o*-An	Ph	*o*-An	65	99
17	(–)	**q**	*o*-An	*o*-An	Ph	40	– [d]

[a] Isolated chemical yield from starting complex **5**. [b] Isolated yield. [c] Not optimized. [d] Air-sensitive ligand used without purification.

When the ring-opened products **6** are treated with a P-chirogenic chlorophosphane borane **8**[60] and then decomplexed with DABCO, the corresponding AMPP ligands **4m**–**p**, featuring additional chirality at the phosphinite fragment, are obtained (Scheme 3, b; Table 1, Entries 13–16). Interestingly, the epimeric P-chirogenic AMPP ligands **4n** and **4o** are obtained by use of the two enantiomers of the *o*-anisylchlorophenylphosphane borane **8**, which are also prepared independently from (+)- or (–)-ephedrine (Table 1, Entries 14, 15).

In addition, the AMPP **4′q** (R^1,R^2 = *o*-An; R^3 = Ph), featuring both P-chirogenic aminophosphane and phosphinite residues, was obtained by the same methodology, but starting from (–)-ephedrine, followed by the trapping of the ring-opened intermediate **6′** with the (*S*)-*o*-anisylchlorophenylphosphane borane **8**[56,60] (Table 1, Entry 17).

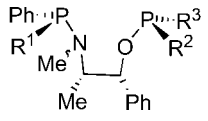

4'

Crystal Structure of the AMPP Diborane 7j

The solid-state structure of the AMPP diborane **7j** was established by X-ray analysis. The compound presents as an unfolded conformation with a flattened nitrogen pyramidal structure and the P–B bonds disposed *anti* from one another (Figure 1). The P1 unit cell contains two independent molecules with similar conformations. The (*S*) absolute configuration of the cyclohexylaminophosphane borane fragment is consistent with the retention of configuration previously reported for the ring-opening cleavage of the starting complex **5**[56,60] on treatment with an organolithium reagent. Interestingly, the C34 and C30 methylene groups point towards the same side of the P–B2 bond, which can be explained by a weaker interaction of the C29–H bond with the methyl C22 located by the nitrogen (Figure 1). Evidence that this methylamino group plays a key role in determining the conformation of the alkyl R^1 substituent in the coordinated AMPP framework is provided below.

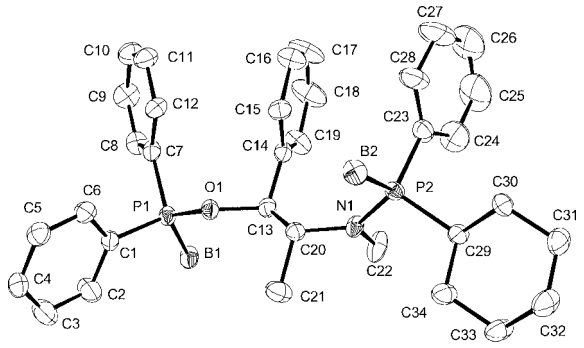

Figure 1. ORTEP representation of AMPP-diborane complex **7j**. For clarity, only one independent molecule is shown. Selected bond lengths [Å], angles [°], and dihedral angles [°] for one of the two molecules: P1–B1 1.904 (2), P2–B2 1.915 (3), P2–N1 1.6697 (17), P1–O1 1.6111 (14); C20–N1–P2 121.83 (13), C22–N1–P2 121.21 (14); C22–N1–C20 116.58 (16), B2–P2–N1–C22 173.99 (18), B2–P2–C23–C28 3.58 (24), O1–C13–C20–N1 172.87 (15), B2–P2–C29–C30 58.63 (18), B2–P2–C29–C34 65.82 (17). The thermal ellipsoids are drawn at 50% probability. The H atoms are not shown for clarity.

Enantioselective Rhodium-Catalyzed Hydrogenations

The AMPP ligands **4a**–**4′q** were used for rhodium-catalyzed asymmetric hydrogenation of the methyl α-acetamidocinnamate **1** (R = Ph; R′, R′′ = Me; Scheme 4), and the results are reported in Table 2 and Table 3.

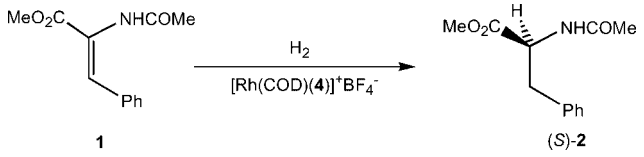

Scheme 4.

When the catalysis was performed in the presence of the EPHOS **4a** in benzene or in CH_2Cl_2, the (*S*)-phenylalanine derivative **2** was obtained with *ee* values of 46 or 11%, respectively (Table 2, Entries 1, 2). Under similar catalytic conditions and in various polar or nonpolar solvents, the ligand AMPP **4b**, bearing an *o*-anisyl group as R^1 substituent, provided the product (*S*)-**2** with 88 to 99% *ee* (Entries 3–7). If the substituent R^1 was *o*-MEMPh, 1-naphthyl, or ferrocenyl (**4c**–**e**), the asymmetric hydrogenation proceeded with *ee* values of 87 to 99% (Entries 8–11), while in the case of the 2-naphthyl or *o*-biphenyl substituents (i.e., **4f**, **4g**), the catalysis gave lower asymmetric induction, the (*S*)-phenylalanine derivative **2** being obtained with only 16% *ee* (Entries 12, 13). On the other hand, when the substituent R^1 was an alkyl group, such as *tert*-butyl, methyl or cyclohexyl, the corresponding AMPP ligands **4h**–**j** afforded either the racemic product or the (*R*) product **2** with *ee* values of 22 and 80%, respectively (Entries 14–16).

Table 2. Rhodium-catalyzed hydrogenation of methyl α-acetamidocinnamate (**1**) in the presence of AMPP ligands **4a**–**j** bearing P-chirogenic aminophosphane fragments.

Entry	AMPP		Conditions[a]		Hydrogenated product **2**		
		R^1	Solvent	Time (h)	Yield (%)[b]	*ee* (%) [c]	Absol. conf.
1	**4a**	Ph	C_6H_6	22	95	46	(*S*)
2	**4a**	Ph	CH_2Cl_2	18	98	11	(*S*)
3	**4b**	*o*-An	C_6H_6	20	98	99	(*S*)
4	**4b**	*o*-An	CH_2Cl_2	10.5	99	89	(*S*)
5	**4b**	*o*-An	MeOH	62.5	91	88	(*S*)
6	**4b**	*o*-An	EtOH	41	95	97	(*S*)
7	**4b**	*o*-An	*i*PrOH	40	94	92	(*S*)
8	**4c**	*o*-MEMPh	C_6H_6	36	94	99	(*S*)
9	**4d**	1-Np	C_6H_6	17	98	95	(*S*)
10	**4d**	1-Np	CH_2Cl_2	4	99	88	(*S*)
11	**4e**	Fc	C_6H_6	47	98	87	(*S*)
12	**4f**	2-Np	CH_2Cl_2	4.5	96	16	(*S*)
13	**4g**	*o*-biPh	C_6H_6	60	95	16	(*S*)
14	**4h**	*t*-Bu	CH_2Cl_2	4	95	2	–
15	**4i**	Me	CH_2Cl_2	3	95	22	(*R*)
16	**4j**	C_6H_{11}	C_6H_6	63	95	80	(*R*)

[a] 0.5 mmol substrate, 3% catalyst, H_2 pressure: 15–20 bar. [b] Isolated yield. [c] Determined by HPLC with a Chiralcel OD column.

Interestingly, in the cases of AMPP ligands **4a**–**j**, each bearing an alkyl or an aryl R^1 substituent on the aminophosphane residue, the catalyzed hydrogenation provided the phenylalanine derivative **2** with either (*R*) or (*S*) absolute configuration.

In addition, the catalysis was also performed with AMPP ligands bearing phosphite or P-chirogenic phosphinite fragments (Table 3). If the diphenylphosphinite residue of the ligand **4a** was changed for a diphenylphosphite, the hydrogenation reaction again afforded the product **2** with the (*S*) configuration, but with 71% *ee* (ligand **4l**; Table 3, Entry 1). In the case in which the AMPP ligand featured a P-chirogenic phosphinite group with *o*-anisyl as R^3 substituent (ligand **4n**), the catalysis gave the hydrogenation product (*S*)-**2** with only 35% *ee* (Entry 2), but the epimeric ligand **4o**,

Table 3. Rhodium-catalyzed hydrogenation of methyl α-acetamidocinnamate (**1**) in the presence of AMPP ligands **4l**–**4′q** bearing phosphite or P-chirogenic phosphinite groups.

Entry	AMPP				Conditions[a]		Hydrogenated product		
		R^1	R^2	R^3	Solvent	Time (h)	Yield (%)[b]	*ee* (%)[c]	Absol. conf.
1	**4l**[d]	*o*-An	OPh	OPh	C_6H_6	24	60	71	(*S*)
2	**4n**	Ph	Ph	*o*-An	C_6H_6	23	96	35	(*S*)
3	**4o**	Ph	*o*-An	Ph	C_6H_6	24	95	62	(*R*)
4	**4o**	Ph	*o*-An	Ph	CH_2Cl_2	85	95	88	(*R*)
5	**4p**	*o*-An	Ph	*o*-An	C_6H_6	21	95	75	(*S*)
6	**4′q**[e]	*o*-An	*o*-An	Ph	CH_2Cl_2	12	94	1	–

[a] 0.5 mmol substrate, 3 mol-% catalyst, H_2 pressure: 15–20 bar. [b] Isolated yield. [c] Determined by HPLC with a Chiralcel OD column. [d] Presence of minor impurity. [e] Prepared from (–)-ephedrine.[56]

with *o*-anisyl as R^2 substituent, provided the product **2** with the (*R*) configuration and with 62 to 88% *ee*, depending on the solvent used (Entries 3, 4). As observed for the ligands **4a**, **4b**, and **4d**, this result confirms increasing induction in favor of either the (*S*) or the (*R*) enantiomer of **2** in benzene or dichloromethane, respectively, as reaction solvents (Table 2, Entries 1–4, 9–10; Table 3, Entries 3, 4). Finally, the ligands **4p** and **4′q**, possessing two P-chirogenic centers with *o*-anisyl as R^1 and R^3 (or R^2) substituents, afforded the hydrogenated product **2** either with (*S*) configuration with 75% *ee*, or in racemic form (Table 3, Entries 5, 6).

Crystal Structure of [Rh(COD)AMPP 4b)]BF_4(9)

The two (+)-ephedrine-derived AMPP ligands **4b** and **4o** afforded both the (*S*) and the (*R*) forms of product **2** with *ee* values of 99 and 88%, respectively (Table 2, Entry 3; Table 3, Entry 4). This result illustrates the importance of the P-center chirality with respect to the ephedrine backbone.

In order to interpret the influence of the chiral rhodium environment on the enantioselectivity, complex **9** was prepared from $[Rh(COD)]_2BF_4$ and the ligand **4b** and then characterized by X-ray crystallography. The crystal structure revealed the existence of two independent molecules with very similar conformations in the unit cell. Figure 2 shows a perspective view of one of the two molecules, together with the numbering scheme. The coordination sphere about the rhodium atom is a distorted square planar structure, with a P1–Rh1–P2 bite angle of 88.54 (4)° and two vertices occupied by the 1,5-cyclooctadiene η^2-bonded

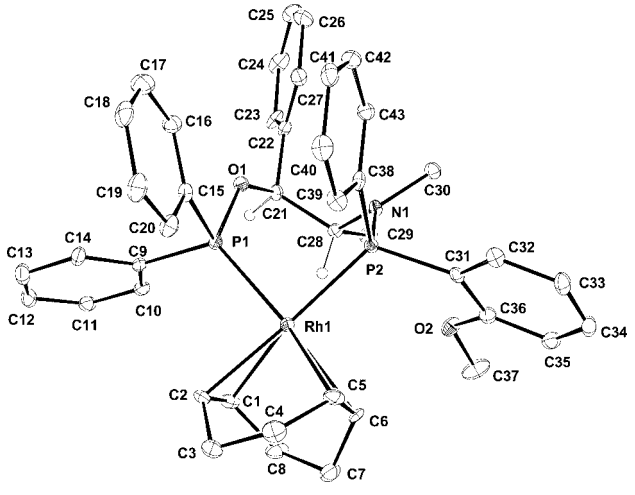

Figure 2. ORTEP representation of the [(COD)Rh(AMPP **4b**)]BF_4 complex **9**. For clarity, only one molecule is shown. Selected bond lengths [Å], angles, and dihedral angles [°] for one of the two molecules: P1–O1 1.619 (3), P2–N1 1.666 (3), P1–Rh1 2.2773 (10), P2–Rh1 2.3229 (10), Rh1–HC28 2.641; P1–Rh2–P2 88.54 (4); O1–P1–P2–N1 21.83 (15), P1–O1–C21–C22 177.96 (23), P1–O1–C28–C29 139.87 (45), phenyl planes C15–C20 and C38–C43 14.00 (21), phenyl–anisyl planes C9–C14 and C31–C36 31.43 (21). The thermal ellipsoids are drawn at 50% probability. The H atoms are not shown for clarity, except for those on the C21 and C28 carbon atoms.

double bonds. The dihedral angles between the planes defined by P1–Rh1–P2 and either C2–Rh1–C6 or C1–Rh1–C5 are 11.02 (12)° and 40.41 (15)°, respectively.

Interestingly, the seven-membered Rh-AMPP chelate ring adopts a boat-like conformation, with a slight distortion of –21.83 (15)° for the O1–P1–P2–N1 dihedral angle, with the substituents of the ephedrine backbone (i.e., Ph, Me) in the equatorial positions. As a consequence, the H–C28 bond points in the direction of the rhodium atom with a H···Rh distance of 2.641 Å. It should be noted that the sum of the angles around the N-atom (i.e., 356.6°) indicates a flattened geometry, which places the C30 methyl group on a side face of the tetrahedral phosphorus center, and in the *anti* position in relation to the P2–Rh bond. This conformation features the C15 and C38 phenyl phosphorus substituents in axial positions, but the distortion of the chelated ring induces an obvious facial dissymmetry for the complex. In addition, the presence of the C30 methyl group and cyclooctadiene ligand forces the methoxy group to be situated at the *anti* position in relation to the P2–C38 axial bond. Finally, the planes of the *o*-anisyl and the C9-phenyl groups form an angle of 31.43°, with both faces oriented toward the metal center.

Model for the Catalyzed Asymmetric Hydrogenation

Metal-chelate rings forming "quasi"-boat structures have also been observed in the cases of RuCpCl[61] and $PdCl_2$[62] complexes of EPHOS **4a** and its modified P-chirogenic derivatives **4e** and **4g**, respectively. This observed conformation was explained by several features. Firstly, the methyl and the phenyl groups situated on the ephedrine backbone were both found in equatorial positions. Secondly, the R^1 group located on the aminophosphane residue is sterically larger than a phenyl one, which favors the equatorial positions. Lastly, the phenyl groups positioned on the two phosphorus atoms do not exhibit intersubstituent interactions at the axial positions, owing to the presence of oxygen and nitrogen atoms on the chelating ring. Simple computer modeling (PC-Model)[63] performed for the model compound Rh(AMPP **4b**)Cl_2 (in the gas phase) has confirmed that this "quasi"-boat structure is more stable than the "quasi"-chair one (by about 10 kJ mol^{-1}).

Although the origin of the catalytic asymmetric induction needs to be carefully explained with the aid of crystal structures,[37,42,54,64] the observation of the same boat conformation regardless of the metal and other ligands (Cl or Cp) used suggests a remarkable stability of this geometry during the catalytic process. Consequently, it may reasonably be assumed that this boat conformation was also retained during the dihydride stereodetermination step.

In order to explain the enantioselectivity of the hydrogenation, a proposed model of the dihydride Rh complex **10** showing the front view as a sextant has been designed (Scheme 5). This model takes account of the boat conformation and the steric and the electronic dissymmetries of the complex in the direction of the cardinal points.

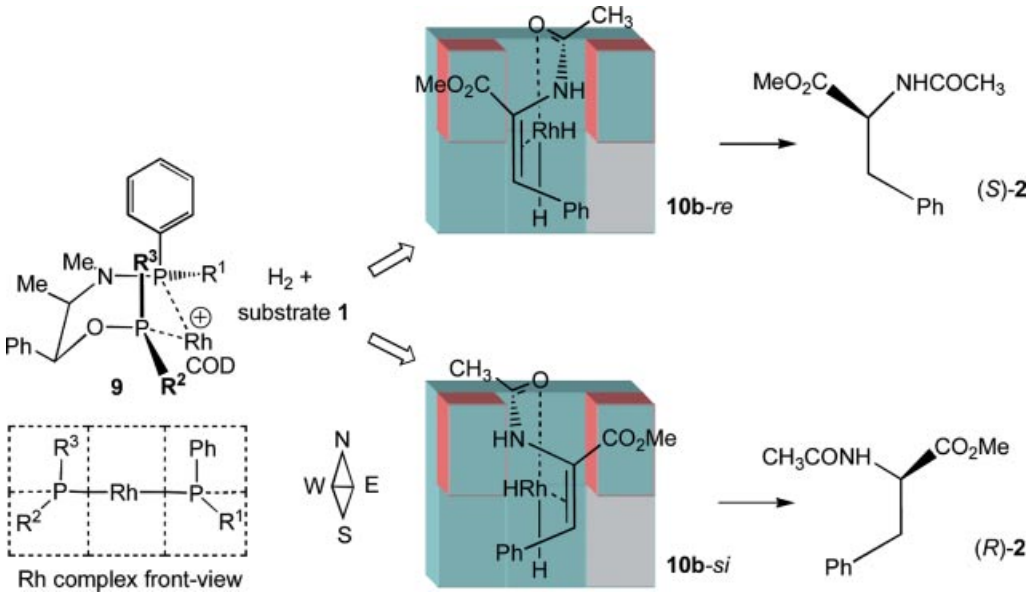

Scheme 5. Only the groups relevant to the Rh–substrate interactions are shown.

From Figure 2 and Scheme 5 it is also easy to see that the coordination of the C=C fragment of the substrate at the north or south positions of the complex **9** produces severe steric hindrance (as verified by computer modeling). Instead, coordination of the C=C on the east or west side of the complex is preferred in this model.

The north-east and north-west parts are thus sterically hindered by the presence of the two axial phenyl phosphorus substituents, almost parallel between them and perpendicular to the complex front view. As the mean distance between these two axial phenyl planes (as crystallographically determined on the rhodium complex **9**) is 3.42 Å, it is likely that the north position could be coordinated only by one hydride or the substrate acetamido group. Computer modeling shows that these axial phenyl groups should easily "open" thanks to the flexibility of the skeleton backbone of the seven-membered ring chelate, to allow coordination of these latter groups onto the Rh metal.

Computer modeling was performed on all four [Rh(AMPP **4b**)H_2 (substrate **1**)] intermediates, with the C=C donor of the substrate coordinated either in the west or in the east positions of the complex (for a total of eight intermediates; the methoxy group of the anisyl substituent was left as is in the structure **9** shown in Figure 2). From molecular distortion arguments (bond lengths and computed energies), two intermediates turned out to be reasonable (**10a**-*re* and **10b**-*re* with the *re* face of the C=C branched on the west side) and these are shown in Figure 3. The most likely nucleophilic attack of the hydride onto the activated substrate should come from that situated parallel to the C=C axis. In such a case the same (*S*) product **2** should be obtained. However, because the computed Rh–C distance in **10b**-*re* is shorter than that of **10a**-*re* (due to steric hindrance), **10b**-*re* is sterically the most likely intermediate, explaining the observed product.

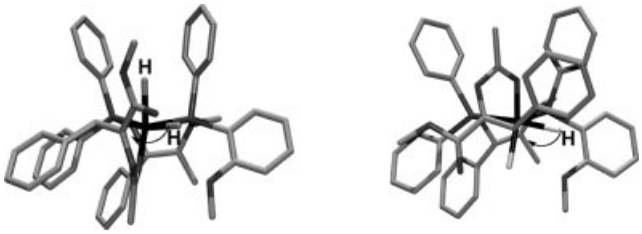

Figure 3. Computer model for the [Rh(AMPP **4b**)H_2 (substrate **1**)] intermediates **10a**-*re* (left) and **10b**-*re* (right) with the C=C branched on the west side, showing plausible hydride nucleophilic attacks on the *re* face of the substrate, both resulting in the same observed (*S*) product **2**.

As many monohydride rhodium-substrate complexes – unlike dihydride rhodium species[38,51] – have been reported in the literature, it appears reasonable to postulate that the intramolecular hydrogen transfer in the intermediates **10** may occur as a fast step. In order to corroborate this hypothesis, the interactions between the substrate and the rhodium dihydride as host complex were analyzed with respect to the observed asymmetric induction.

Thus, when R^1 is a larger aryl group (i.e., than a phenyl), the dissymmetry in the east-west region of the rhodium complex is amplified, which must promote the coordination of the cinnamyl group on the west part and on its *re* face (Scheme 5). A facile hydrogen insertion could therefore occur between the two aryl planes (i.e., the phenyl group of the cinnamyl and the R^1 group) to provide the intermediate **10b**-*re* as major product. This model explains why all the results obtained for the EPHOS **4a** and its derivatives **4b**–**g** involve the (*S*)-phenylalanine derivative **2** (Table 2, Entries 2–13). On this basis, when the steric hindrance of the R^1 aryl group is increased, the coordination of the cinnamyl in the west region of the intermediate **10b**-*re*, and conse-

quently the asymmetric induction towards the (*S*) enantiomer, is still more favored. Whereas good to excellent *ee* values were obtained with the AMPP ligands **4b**–**e** (R^1 = *o*-An, *o*-MEMPh, 1-Np, Fc), the lower asymmetric induction observed in the case of ligands **4f** and **4g** could be explained in terms of similar plane conformation of the 2-naphthyl or biphenyl substituents with regard to the phenyl group, producing results comparable to those obtained with EPHOS **4a** (Table 2, Entries 1, 12, 13).

On the other hand, when the AMPP ligand **4** bears an alkyl group as the R^1 substituent, the insertion of the hydrogen between the cinnamyl and this group is now disfavored for steric reasons, resulting in the coordination of the substrate on the east region and its *si* face, as illustrated in the case of the intermediate **10b**-*si* (Scheme 5, Scheme 6). In this case, the steric interactions with the CH vinylic group must be weaker. It should be noted that the methyl C30 group located on the amino residue, which occupies the *anti* position in relation to the P2–Rh bond, probably contributes to the steric hindrance by forcing the alkyl R^1 group to be located on the front side of the complex (Figure 2, Scheme 6). These steric effects explain why the methyl- and cyclohexyl-containing AMPP ligands **4i** and **4j** provide the phenylalanine derivative (*R*)-**2** with *ee* values of 22 and 88%, respectively (Table 2, Entries 15, 16). Computer modeling using the R^1 = Me group (instead of anisyl), for example, confirms this trend. Indeed, the two most probable intermediate structures (from the lowest computed energy) promote both the (*S*) (**10 b**-*re*; most stable) and (*R*) (**10b**-*si*; second most stable) products (Figure 4). However, the relative orientation of the hydride with respect to the olefin is a little better for the intermediate (**10b**-*si*) that provides the (*R*) product. All in all, these findings corroborate the experimental results.

When R^1 was a *tert*-butyl group, however, no asymmetric induction was observed (Table 2, Entry 14). In this last case, it is plausible that the two dihydride rhodium intermediates **10b**-*re* and **10b**-*si* are both equally disfavored, owing to steric interactions of the *tert*-butyl group with either the ester or the cinnamyl moiety in the east region (Scheme 6).

In addition, when the ligand is substituted with phenoxy groups in the R^2 and R^3 positions (ligand **4l**), the east-west dissymmetry of the complex remains similar to that of the AMPP ligands **4a**–**g**, because the steric hindrance of the diphenylphosphonite and diphenylphosphinite are closed. Consequently, substrate coordination in the west region is again favored, to afford the intermediate **10b**-*re* and the (*S*) product **2** (Scheme 5; Table 3, Entry 1). If the AMPP ligand now bears an *o*-anisyl group as R^3 substituent, the catalyzed hydrogenation again affords the (*S*) product **2**, but with only 35% *ee* (ligand **4n**, Table 3, Entry 2). The weak influence of the substitution at this R^3 position could be explained by the *o*-anisyl conformation, the methoxy group being positioned at the back side of the phosphorus-metal bond, thus affording steric hindrance comparable with that of a phenyl group at the front side of the catalytic site. This result is in good agreement with those obtained with the ligand EPHOS **4a**, also bearing two phenyl groups at the R^1 and R^3 positions (46% *ee*; Table 2, Entry 1). Moreover, this result also compares favorably with those obtained with the ligands **4b** (R^1 = *o*-An, R^3 = Ph) and **4p** (R^1 = *o*-An, R^3 = *o*-An), which provide the (*S*) product **2** with 99% and 75% *ee*, respectively (Table 2, Entry 3; Table 3, Entry 5). Finally, all these results demonstrate the strong influence of the substitution at the R^1 position on the enantioselectivity, whereas the R^3 substituents (at least in the case of an *o*-anisyl substituent) play a secondary role. It should be noted that the difference in the influence of R^1 and R^3 would be more difficult to explain with the quadrant rule.

In the case of the AMPP **4′q**, in which R^1 and R^2 are two *o*-anisyl groups, the front view dissymmetry of the rhodium complex is then lost, resulting in equal coordination of the substrate to the *re* and *si* faces affording no asymmetric induction (Table 3, Entry 6). However, if the *o*-anisyl group occupies only the R^2 position, as in the ligand **4o**, the dissymmetry of the complex east-west region is then opposite. This then results in the coordination of the cinnamate on the east side and its *si*-face, as shown by the intermediate **10b**-*si* (Scheme 5), the phenylalanine derivative **2** then being

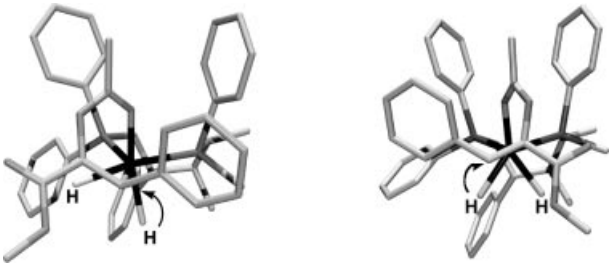

Figure 4. Computer model for the [Rh(AMPP **4i**)H_2 (substrate **1**)] intermediates **10b**-*re* (left) and **10b**-*si* (right) with C=C branched on the east and west sides, respectively, showing plausible hydride nucleophilic attacks on the C=C bond, both resulting in the (*S*) and the (*R*) product **2**, respectively.

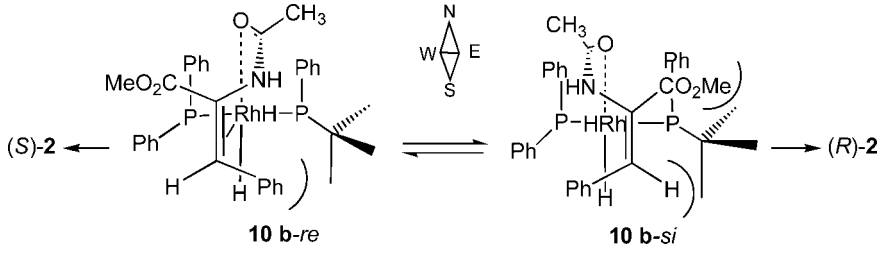

Scheme 6.

obtained with the (*R*) absolute configuration and with *ee* values reaching 88% (Table 3, Entries 3, 4).

Conclusions

A new series of P-chirogenic aminophosphane-phosphinite ligands (AMPP) **4** has been synthesized from (+)- or (–)-ephedrine by a versatile three-step methodology. The AMPP ligands **4a**–**4′q** were used in the forms of their rhodium complexes for catalyzed hydrogenations of methyl α-acetamidocinnamate **1** as a test reaction. Notably, although all the AMPP ligands **4a**–**4p** derive from the (+)-ephedrine backbone, variation of the substituent on a P-center could result in the catalyzed hydrogenation product **2** with either (*R*) or (*S*) absolute configurations, with *ee* values ranging from 99% (*S*) to 88% (*R*). Indeed, it is particularly interesting to optimize an asymmetric catalysis of a designed target by use of a modular approach such as those presented for the EPHOS AMPP ligand **4a**. The asymmetric induction was analyzed in the light of X-ray structures of the AMPP **4** complexes, and a new model for the enantioselectivity, taking into consideration both the boat conformation and the steric and the electronic dissymmetries of the complex, has been proposed. This model offers an alternative to the quadrant rule well adapted to the C_2-symmetry ligands and the twisted-chair conformations of their complexes. In this work, the model – which schematizes the front side of the complex as a sextant in the direction of the cardinal points – is consistent with complexation of the substrate by the acetamido and the cinnamyl groups, in the north and east (or west) parts, respectively. The enantioselectivity is due to the nature of the ligand substituents in the south-east or south-west parts of the key substrate-dihydride intermediate. Further developments to extend the catalyzed asymmetric hydrogenation for pharmaceutical targets and DFT calculations on the stereochemical course of the dihydride-Rh-substrate complex are in progress.

Experimental Section

General: All reactions were carried out under argon in dried glassware. Solvents were dried and freshly distilled under argon and over sodium/benzophenone for THF, diethyl ether, toluene, and benzene, over P_2O_5 for CH_2Cl_2, and over sodium ethoxide for EtOH. Hexane and propan-2-ol for HPLC were of chromatography grade and were used without further purification. Methyllithium, *sec*-butyllithium, *tert*-butyllithium, ferrocene, chlorodiphenylphosphane, and chlorodicyclohexylphosphane were purchased from Aldrich, Acros, and Avocado and used as received. Commercially available 2-bromoanisole, and bromobenzene were distilled before use, whereas 1-bromonaphthalene, 2-bromonaphthalene, 2-bromobiphenyl, and bromocyclohexane were used without purification. The HCl in toluene solution was obtained by bubbling HCl gas and titration of the resulting solution by colorimetry. The (2*S*,4*R*,5*S*)-(–)-3,4-dimethyl-2,5-diphenyl-1,3,2-oxazaphospholidine-2-borane (**5**) and its enantiomer,[59] (*S*)-(–)- and (*R*)-(+)-*o*-anisyl(chloro)-phenylphosphane–borane **8**, the AMPP ligands **4a**, **4b**, **4d**, **4f**, **4h**, **4i**, **4k**, **4m**, and **4q**, and their corresponding diborane complexes **7** were prepared from the appropriate (+)- or (–)-ephedrine as described previously.[56]

HPLC analyses were performed on a Gilson and Shimadzu apparatus fitted with a UV detector. The enantiomeric excesses of the optically active derivatives were determined on Chiralcel OD or OK columns (Daicel), with hexane/*i*PrOH mixtures as the mobile phase, a flow rate of 1 mL min^{-1} and UV detection at λ = 254 and 280 nm. Thin-layer chromatography was performed on silica chromagel (60 F_{254}; SDS) and results were viewed by UV, potassium permanganate, or iodine treatment. Flash chromatography was performed on silica gel (60ACC, 6–35 microns and 35–70 microns; SDS). All NMR spectra data were recorded on Bruker DPX 250 or Advance 300–500 spectrometers with TMS as internal reference for ^{1}H and ^{13}C NMR and 85% phosphoric acid as external reference for ^{31}P NMR spectroscopy. Melting points were measured on a Büchi 530 melting point apparatus and are uncorrected. Optical rotations were determined at 20 °C on Perkin–Elmer 241 and 341 polarimeters. Infrared spectra were recorded on Bruker Equinox 55 and Vector 22 instruments. Mass spectral analyses were performed on NERMAG R10-10C and on JEOL MS 700 and KRATOS Concept S instruments at the ENSCP (Paris), ENS (Paris), and Burgundy University (Dijon), respectively. The major peak *m*/*z* was mentioned with the intensity as a percentage of the base peak in brackets. Elemental analyses were measured with a precision superior to 0.3% at the Microanalysis Laboratories of P. & M. Curie (Paris) and Burgundy (Dijon) Universities.

Preparation of 1-Bromo-2-{[(2-methoxy)ethoxy]methoxy}benzene: This compound was prepared by a modified procedure described previously.[65] NaH (60% in mineral oil, 1.40 g, 35 mmol) was placed in a three-necked flask fitted with a magnetic stirrer and washed twice with pentane. Dry THF (10 mL) was then added, the mixture was cooled to 0 °C, and 2-bromophenol (3.0 mL, 26 mmol) was slowly added with stirring. The mixture was stirred for 2 h at 0 °C, and chloro{[(2-methoxy)ethoxy]methane (3.0 mL, 26 mmol) was slowly added. The mixture was stirred for 30 min at 0 °C and allowed to warm to room temperature overnight. THF was evaporated under reduced pressure and the residue was hydrolyzed at room temperature and extracted with CH_2Cl_2. The organic extracts were dried with anhydrous $MgSO_4$ and the solvent was removed under vacuum. The residue was purified by chromatography on silica gel with diethyl ether/petroleum ether (1:3) as eluent, yielding the product (5.83 g, 86%) as a colorless oil. R_f = 0.3 (diethyl ether/petroleum ether, 1:3). ^{1}H NMR ($CDCl_3$): δ = 3.37 (s, 3 H, CH_3O), 3.57 (m, 2 H, CH_2O), 3.88 (m, 2 H, CH_2O), 5.34 (s, 2 H, OCH_2O), 6.89 (dt, *J* = 1.6, *J* = 7.6 Hz, 1 H, *H* arom.), 7.19–7.27 (m, 2 H, *H* arom.), 7.54 (dd, *J* = 1.6, *J* = 7.9 Hz, 1 H, *H* arom.) ppm. ^{13}C NMR ($CDCl_3$): δ = 58.80 (*C*H$_3$), 67.86 (*C*H$_2$), 71.34 (*C*H$_2$), 93.91 (*C*H$_2$), 112.64 (*C*Br), 116.13 (*C* arom.), 122.96 (*C* arom.), 128.33 (*C* arom.), 133.17 (*C* arom.), 153.60 (*C*O arom.) ppm. IR (neat, $\tilde{\nu}$): 3069–2883, 1585, 1474, 1275, 1230, 1159, 1101, 1037, 976, 848, 750 cm^{-1}. MS (EI): *m*/*z* (%) = 262 (40) [M]$^+$, 260 (40) [M]$^+$, 187 (35), 185 (35), 174 (45), 172 (45), 157 (35), 155 (35), 145 (20), 143 (20), 89 (85), 59 (100). HRMS (EI) calcd. for $C_{10}H_{13}O_3{}^{81}Br$ [M]$^+$: 262.00276; found: 262.00552. $C_{10}H_{13}O_3Br$ (261.116): C 46.00, H 5.02; found: C 46.33, H 5.16.

Transmetalation of 1-Bromo-2-{[(2-methoxy)ethoxy]methoxy}-benzene: The bromo derivative (1 equiv.) was placed in a two-necked flask fitted with a magnetic stirrer. The mixture was cooled to 0 °C and *sec*-butyllithium (1 equiv.) was slowly added by syringe and with stirring. After the formation of a white precipitate, the mixture was stirred for 1 h at 0 °C. The organolithium reagent was dissolved with a minimum of THF before use.

Preparation of the Aminophosphane-Phosphinite Diboranes 7. General Procedure for AMPP Ligands 7a–k: A 100 mL round-bottomed flask fitted with a magnetic stirrer and an argon inlet was charged with oxazaphospholidine borane **5** (1 equiv., 3.5 mmol) and THF (6 mL). An organolithium reagent[66] (2 equiv., 7 mmol) was added slowly at –78 °C with stirring, the reaction temperature was allowed to rise slowly to 0 °C, and stirring was maintained until complex **5** had disappeared completely. Chlorophosphane (2 equiv., 7 mmol) was added and the mixture was stirred for 2 h and allowed to warm to room temperature. Borane–dimethyl sulfide (BMS, 10 equiv.) was added and the mixture was stirred overnight. BMS and THF were evaporated under reduced pressure and the residue was hydrolyzed at room temperature and then extracted with CH_2Cl_2. The organic extracts were dried with anhydrous $MgSO_4$ and the solvent was removed. The residue was purified by chromatography on silica gel with toluene/petroleum ether (1:1) as eluent, yielding the AMPP diborane **7**, which was then recrystallized from a CH_2Cl_2/hexane mixture.

AMPP 7l: This AMPP diborane complex was prepared by a modification of the procedure described above with use of triphenylphosphite instead of the chlorophosphane. After workup and chromatography, the ligand was used without further purification.

AMPP Ligands 7m–q: The AMPP diboranes **7m–q** were obtained by a modification of the procedure described above with use of the corresponding P-chirogenic chlorophosphane borane **8**[56,60] instead of the chlorodiphenylphosphane.

(*R*p)-(–)-{[(1*R*,2*S*)-2-(Diphenylphosphinito–borane)-1-methyl-2-phenylethyl](methyl)amino}{*o*-[(2-methoxyethoxy)methoxy]phenyl}-phosphane–Borane (7c): 1.62 g (66%); white crystals (CH_2Cl_2/hexane); m.p. 95 °C. $[a]_D^{20}$ = –51 (*c* = 1, $CHCl_3$); R_f = 0.2 (toluene/AcOEt, 98:2). ^{1}H NMR ($CDCl_3$): δ = 0.20–1.60 (m, 6 H, B*H*$_3$), 1.32 (d, $^3J_{HH}$ = 6.5 Hz, 3 H, C*H*$_3$), 2.34 (d, $^3J_{PNCH}$ = 7.7 Hz, 3 H, NC*H*$_3$), 3.23 (s, 3 H, OC*H*$_3$), 3.34 (m, 4 H, OC*H*$_2$), 4.35–4.70 (m, 1 H, C*H*N), 4.77 (d, *J* = 7.1 Hz, 1 H, OC*H*$_2$O), 4.84 (d, *J* = 7.1 Hz, 1 H, OC*H*$_2$O), 5.23 (t, *J* = 9.2 Hz, 1 H, C*H*O), 6.54–6.63 (m, 2 H, *H* arom.), 6.90–7.30 (m, 15 H, *H* arom.), 7.31–7.47 (m, 5 H, *H* arom.), 7.60–7.68 (m, 2 H, *H* arom.) ppm. ^{13}C NMR ($CDCl_3$): δ = 15.9 (*C*H$_3$), 29.8 (d, $^2J_{PNC}$ = 4.7 Hz, NC*H*$_3$), 56.9 (dd, $^2J_{PNC}$ = 8.8, $^3J_{POCC}$ = 11.7 Hz, NC*H*), 58.9 (OC*H*$_3$), 67.7 (OC*H*$_2$), 71.3 (OC*H*$_2$), 83.8 (dd, J_{PC} = 2.7, J_{PC} = 8.6 Hz, OC*H*), 93.2 (OC*H*$_2$O), 114.5 (d, J_{PC} = 4.4 Hz, *C* arom.), 118.8 (d, J_{PC} = 56.1 Hz, *C* arom.), 121.9 (d, J_{PC} = 10.5 Hz, *C* arom.), 127.7 (d, J_{PC} = 10.9 Hz, *C* arom.), 127.8 (d, J_{PC} = 10.6 Hz, *C* arom.), 128.0 (*C* arom.), 128.4 (d, J_{PC} = 7.7 Hz, *C* arom.), 128.6 (*C* arom.), 128.7 (*C* arom.), 129.5 (d, J_{PC} = 2.3 Hz, *C* arom.), 130.4 (d, J_{PC} = 10.8 Hz, *C* arom.), 131.0 (d, J_{PC} = 11.1 Hz, *C* arom.), 131.9–132.3 (*C* arom.), 132.8 (*C* arom.), 133.4 (d, J_{PC} = 1.5 Hz, *C* arom.), 134.9 (d, J_{PC} = 11.0 Hz, *C* arom.), 137.9 (*C* arom.), 159.0 (d, J_{PC} = 2.2 Hz, *C* arom.) ppm. ^{31}P NMR ($CDCl_3$): δ = 69.9 (br, *P*-N), 108.0 (br, *P*-O) ppm. IR (neat): $\tilde{\nu}$ = 3065–2817, 2394, 2374, 2342, 1586, 1573, 1473, 1457, 1435, 1438, 1434, 1308, 1269, 1242, 1226, 1201, 1163, 1154, 1132, 1100, 1087, 1076, 1055, 1031, 1009, 999, 984, 965, 924, 895, 873, 854, 846, 797, 765, 743, 733, 727, 709, 695; 653, 620, 607 cm^{-1}. $C_{38}H_{47}B_2NO_4P_2 \cdot 2H_2O$ (701.397): C 65.07, H 7.33, N 2.00; found: C 65.41, H 7.34, N 2.47.

Compound 7e: 1.45 g (62%); orange crystals (CH_2Cl_2/hexane); m.p. 170–171 °C. $[a]_D^{20}$ = +45.6 (*c* = 1, $CHCl_3$); R_f = 0.2 (toluene/petroleum ether, 1:1). ^{1}H NMR ($CDCl_3$): δ = 0.20–1.60 (m, 6 H, B*H*$_3$), 1.25 (d, $^3J_{HH}$ = 6.5 Hz, 3 H, C*H*$_3$), 1.99 (d, $^3J_{HP}$ = 8.0 Hz, 3 H, NC*H*$_3$), 3.96 (br, 1 H, Cp), 4.19 (s, 5 H, Cp), 4.34 (br, 1 H, Cp), 4.40 (br, 1 H, Cp), 4.45 (m, 1 H, C*H*N), 4.50 (br, 1 H, Cp), 5.23 (t, *J* = 9.1 Hz, 1 H, C*H*O), 6.80–6.88 (m, 2 H, *H* arom.), 6.95–7.10 (m, 7 H, *H* arom.), 7.13–7.30 (m, 6 H, *H* arom.), 7.32–7.50 (m, 3 H, *H* arom.), 7.60–7.70 (m, 2 H, *H* arom.) ppm. ^{13}C NMR ($CDCl_3$): δ = 15.8 (*C*H$_3$), 29.0 (d, $^2J_{PNC}$ = 4.0 Hz, NC*H*$_3$), 56.9 (dd, $^2J_{PNC}$ = 9.0, $^3J_{POCC}$ = 10.2 Hz, NC*H*), 70.2 (Cp), 70.6 (Cp), 70.9 (d, J_{PC} = 6.2 Hz, Cp), 71.1 (d, J_{PC} = 8.3 Hz, Cp), 71.5 (Cp), 72.0 (d, J_{PC} = 8.8 Hz, Cp), 72.1 (Cp), 83.4 (dd, $^2J_{POC}$ = 2.8, $^3J_{PNCC}$ = 9.3 Hz, OC*H*), 127.8 (d, J_{PC} = 5.5 Hz, *C* arom.), 127.9 (d, J_{PC} = 5.4 Hz, *C* arom.), 128.0 (*C* arom.), 128.3 (d, J_{PC} = 13.0 Hz, *C* arom.), 128.5 (*C* arom.), 128.6 (*C* arom.), 130.1 (d, J_{PC} = 2.1 Hz, *C* arom.), 130.9–131.6 (*C* arom.), 131.8 (*C* arom.), 132.1 (d, J_{PC} = 6.2 Hz, *C* arom.), 132.8 (*C* arom.), 138.2 (*C* arom.) ppm. ^{31}P NMR ($CDCl_3$): δ = 71.8 (br, *P*-N), 107.8 (d, $^1J_{PB}$ = 58.0 Hz, *P*-O) ppm. IR (neat): $\tilde{\nu}$ = 3053–2930, 2383, 2348, 1483, 1457, 1435, 1224, 1205, 1167, 1131, 1108, 1064, 1027, 1006, 988, 963, 898, 866, 825, 762, 734, 715, 697 cm^{-1}. MS (EI): *m*/*z* (%) = 669 (2) [M]$^+$, 452 (10), 387 (5), 293 (100), 226 (5), 186 (25), 107 (5). $C_{38}H_{43}B_2NOP_2Fe$ (669.183): C 68.21, H 6.48, N 2.09; found: C 67.85, H 6.60, N 2.88.

Compound 7g: 0.89 g (40%); colorless crystals (CH_2Cl_2/hexane); m.p. 159–160 °C. $[a]_D^{20}$ = –79.2 (*c* = 1, $CHCl_3$); R_f = 0.3 (toluene/petroleum ether, 1:1). ^{1}H NMR ($CDCl_3$): δ = 0.20–1.60 (m, 6 H, B*H*$_3$), 1.10 (d, $^3J_{HH}$ = 6.6 Hz, 3 H, C*H*$_3$), 2.30 (d, $^3J_{HP}$ = 7.0 Hz, 3 H, NC*H*$_3$), 4.32 (m, 1 H, C*H*N), 5.33 (t, *J* = 8.6 Hz, 1 H, C*H*O), 6.43–6.78 (m, 3 H, *H* arom.), 6.87–7.02 (m, 12 H, *H* arom.), 7.02–7.16 (m, 6 H, *H* arom.), 7.28–7.39 (m, 6 H, *H* arom.), 7.54–7.60 (m, 2 H, *H* arom.) ppm. ^{13}C NMR ($CDCl_3$): δ = 14.6 (d, $^3J_{PNCC}$ = 2.3 Hz, *C*H$_3$), 29.9 (d, $^2J_{PNC}$ = 3.5 Hz, NC*H*$_3$), 57 (dd, $^2J_{PNC}$ = 8.4, $^3J_{POCC}$ = 10.3 Hz, NC*H*), 82.5 (m, OC*H*), 126.8–127.1 (*C* arom.) 127.7 (d, J_{PC} = 2.1 Hz, *C* arom.), 127.7 (d, J_{PC} = 26.3 Hz, *C* arom.) 128.5 (d, J_{PC} = 10.9 Hz, *C* arom.), 129.2 (*C* arom.), 129.8 (*C* arom.), 130.0 (d, J_{PC} = 2.1 Hz, *C* arom.), 130.3 (d, J_{PC} = 1.9 Hz, *C* arom.), 130.5 (*C* arom.), 131.0 (d, J_{PC} = 11.2 Hz, *C* arom.), 131.2 (d, J_{PC} = 2.1 Hz, *C* arom.), 131.3 (*C* arom.), 131.5 (d, J_{PC} = 11.6 Hz, *C* arom.), 131.5 (d, J_{PC} = 2.4 Hz, *C* arom.), 131.8 (d, J_{PC} = 15.2 Hz, *C* arom.), 132.0 (d, J_{PC} = 22.9 Hz, *C* arom.) 132.7 (*C* arom.), 132.8 (d, J_{PC} = 8.2 Hz, *C* arom.), 133.3 (d, J_{PC} = 9.4 Hz, *C* arom.), 137.6 (*C* arom.), 140.7 (d, J_{PC} = 2.7 Hz, *C* arom.), 146.9 (d, J_{PC} = 10.4 Hz, *C* arom.) ppm. ^{31}P NMR ($CDCl_3$): δ = 72.4 (br, *P*-N), 107.2 (d, $^1J_{PB}$ = 69.9 Hz, *P*-O) ppm. IR (neat): $\tilde{\nu}$ = 3056–2910, 2425, 2400, 2376, 2336, 1587, 1481, 1457, 1448, 1437, 1223, 1161, 1108, 1058, 1011, 999, 987, 965, 894, 860, 758, 736, 712, 694, 689, 621, 605 cm^{-1}. MS (LSIMS): *m*/*z* (%) = 636.1 [M – H]$^+$ (7), 408.1 (15), 318.1 (50), 261.0 (95), 183 (100). $C_{40}H_{43}B_2NOP_2$ (637.358): C 75.38, H 6.80, N 2.20; found: C 75.59, H 6.88, N 2.81.

Compound 7j: 0.75 g (38%); colorless crystals (CH_2Cl_2/hexane); m.p. 127–128 °C. $[a]_D^{20}$ = –42.7 (*c* = 0.4, $CHCl_3$); R_f = 0.56 (toluene/petroleum ether, 1:1). ^{1}H NMR ($CDCl_3$): δ = 0.20–1.20 (m, 9 H), 1.35 (d, $^3J_{HH}$ = 6.6 Hz, 3 H, C*H*$_3$), 1.30–1.86 (m, 7 H), 2.18 (m, 1 H, PC*H*), 2.39 (d, $^3J_{HP}$ = 6.7 Hz, 3 H, NC*H*$_3$), 4.27 (m, 1 H, C*H*N), 5.40 (dd, *J* = 9.2 Hz, 1 H, C*H*O), 6.75–7.15 (m, 11 H, *H* arom.), 7.22–7.30 (m, 4 H, *H* arom.), 7.40–7.60 (m, 3 H, *H* arom.), 7.68–7.72 (m, 2 H, *H* arom.) ppm. ^{13}C NMR ($CDCl_3$): δ = 15.8 (d, J_{PNCC} = 1.4 Hz, *C*H$_3$), 25.9 (d, J_{PC} = 1.4 Hz, *C*H$_2$), 26.0 (*C*H$_2$), 26.6 (d, J_{PC} = 7.6 Hz, *C*H$_2$), 26.7 (d, J_{PC} = 1.9 Hz, *C*H$_2$), 26.9 (d, J_{PC} = 11.9 Hz, *C*H$_2$), 28.0 (d, $^2J_{PNC}$ = 3.4 Hz, NC*H*$_3$), 32.7 (d, $^1J_{PC}$ = 43.1 Hz, *C*H), 57.7 (dd, $^2J_{PNC}$ = 8.6 Hz, NC*H*), 82.8 (dd, $^3J_{PNCC}$ = 4.3, $^2J_{POC}$ = 3.1 Hz, OC*H*), 125.2 (*C* arom.), 127.6–128.2 (*C* arom.), 128.5 (d, J_{PC} = 10.9 Hz, *C* arom.), 129.0 (*C* arom.), 129.7 (*C* arom.), 130.0 (d, J_{CP} = 2.0 Hz, *C* arom.), 130.4 (*C* arom.), 130.8 (d, J_{PC} = 9.3 Hz, *C* arom.), 131.0 (d, J_{PC} = 11.2 Hz, *C* arom.), 131.2–131.6 (*C* arom.), 131.9 (d, J_{PC} = 23.7 Hz, *C* arom.), 132.7 (*C* arom.), 137.8 (*C* arom.) ppm. ^{31}P NMR ($CDCl_3$): δ = 74.6 (d, $^1J_{PB}$ = 60.5 Hz, *P*-N), 107.7 (d, $^1J_{PB}$ = 64.9 Hz, *P*-O) ppm. IR (neat): $\tilde{\nu}$

= 3064, 2932, 2855, 2393, 2348, 1451, 1437, 1223, 1132, 1113, 1065, 1016, 967, 920, 895, 861, 768, 756, 734, 710, 687, 623 cm^{-1}. $C_{34}H_{45}B_2NOP_2$ (567.308): C 71.98, H 8.00, N 2.47; found: C 71.84, H 8.50, N 2.48.

Compound 7l: 0.65 g (30%); colorless, viscous oil; R_f = 0.45 (toluene). ^1H NMR ($CDCl_3$): δ = 0.20–1.20 (m, 6 H), 1.31 (d, $^3J_{HH}$ = 6.6 Hz, 3 H, CH_3), 2.52 (d, $^3J_{PNCH}$ = 8.0 Hz, 3 H, NCH_3), 3.55 (s, 1 H, OCH_3), 4.59 (m, 1 H, C*H*N), 5.72 (t, J = 8.0 Hz, 1 H, C*H*O), 6.75–7.65 (m, 24 H, *H* arom.) ppm. ^{31}P NMR ($CDCl_3$): δ = 71.6 (br, *P*-N), 113.3 (br, *P*-O) ppm. The presence of a minor impurity was detected at δ = 69.5 ppm.

Compound 7n: 1.14 g (55%); white crystals (CH_2Cl_2/hexane); m.p. 165 °C. $[\alpha]_D^{20}$ = –71.1 (c = 1.3, $CHCl_3$); R_f = 0.55 (toluene). ^1H NMR ($CDCl_3$): δ = 0.30–1.80 (br, 6 H, BH_3), 1.24 (d, $^3J_{HH}$ = 6.8 Hz, 3 H,CH_3), 2.21 (d, $^3J_{PNCH}$ = 7.6 Hz, 3 H, NCH_3), 3.46 (s, 3 H, OCH_3), 4.50 (m, 1 H, C*H*N), 5.33 (t, J = 9.4 Hz, 1 H, C*H*O), 6.50–6.58 (m, 2 H, *H* arom.), 6.76 (dd, $^3J_{HH}$ = 8.3, $^3J_{PCCH}$ = 4.7 Hz, 1 H, *H* arom.), 6.90–7.50 (m, 20 H, *H* arom.), 7.75–7.85 (m, 1 H, *H* arom.) ppm. ^{13}C NMR ($CDCl_3$): δ = 16.1 (*C*H_3), 29.5 (d, $^2J_{PNC}$ = 4.5 Hz, N*C*H_3), 55.6 (O*C*H_3), 57.7 (dd, $^3J_{POCC}$ = 11.0, $^2J_{PNC}$ = 8.4 Hz, N*C*H), 82.5 (dd, $^3J_{PNCC}$ = 8.9, $^2J_{POC}$ = 2.6 Hz, O*C*H), 111.9 (d, J_{PC} = 5.3 Hz, *C* arom.), 120.3 (d, J_{PC} = 70.3 Hz, *C* arom.), 120.9 (d, J_{PC} = 10.5 Hz, *C* arom.), 127.5 (d, J_{PC} = 10.9 Hz, *C* arom.), 128.0–129.4 (*C* arom.), 130.3–131.3 (*C* arom.), 131.8 (d, J_{PC} = 10.3 Hz, *C* arom.), 132.6 (d, J_{PC} = 10.3 Hz, *C* arom.), 132.7 (d, J_{PC} = 62.3 Hz, *C* arom.), 133.4 (d, J_{PC} = 9.4 Hz, *C* arom.), 134.0 (d, J_{PC} = 2.5 Hz, *C* arom.), 138.5 (*C* arom.), 161.0 (d, J_{PC} = 4.3 Hz, *C* arom.) ppm. ^{31}P NMR ($CDCl_3$): δ = 72.4 (br, *P*-N), 106.6 (br, *P*-O) ppm. IR (neat): $\tilde{\nu}$ = 3093–2898, 2385, 2345, 1478, 1455, 1436, 1253, 1159, 1134, 1111, 1060, 1009, 979, 893, 864, 755, 737, 724, 694 cm^{-1}. MS (EI): *m*/*z* (%) = 590 (20) $[M – H]^+$, 586 (40), 576 (100), 563 (45), 529 (20), 506 (50), 487 (35), 471 (20), 458 (20), 441 (15), 431 (20), 417 (20), 400 (25), 390 (20), 360 (20), 348 (25), 332 (40), 276 (30), 242 (85), 181 (85), 141 (100), 91 (45). $C_{35}H_{41}B_2NO_2P_2$ (591.238): C 71.10, H 6.99, N 2.37; found: C 71.10, H 7.26, N 2.48.

Compound 7o: 1.14 g (55%); white crystals (CH_2Cl_2/hexane); m.p. 170 °C. $[\alpha]_D^{20}$ = –98.5 (c = 1.4, $CHCl_3$); R_f = 0.55 (toluene). ^1H NMR ($CDCl_3$): δ = 0.30–1.80 (br, 6 H, BH_3), 1.41 (d, $^3J_{HH}$ = 6.5 Hz, 3 H, CH_3), 2.31 (d, $^3J_{PNCH}$ = 7.6 Hz, 3 H, NCH_3), 3.37 (s, 3 H, OCH_3), 4.63 (m, 1 H, C*H*N), 5.37 (t, J = 9.2 Hz, 1 H, C*H*O), 6.40–6.85 (m, 4 H, *H* arom.), 7.00–7.15 (m, 5 H, *H* arom.), 7.20–7.80 (m, 15 H, *H* arom.) ppm. ^{13}C NMR ($CDCl_3$): δ = 16.3 (*C*H_3), 29.5 (N*C*H_3), 54.8 (O*C*H_3), 57.6 (m, N*C*H), 82.3 (m, O*C*H), 110.5 (*C* arom.), 118.9 (d, J_{PC} = 55.1 Hz, *C* arom.), 120.0 (d, J_{PC} = 11.3 Hz, *C* arom.), 128.1–133.3 (*C* arom.), 134.3 (*C* arom.), 135.4 (d, J_{PC} = 16.6 Hz, *C* arom.), 138.0 (*C* arom.), 160.5 (*C* arom.) ppm. ^{31}P NMR ($CDCl_3$): δ = 72.2 (br, *P*-N), 105.1 (br, $^1J_{PB}$ = 52.4 Hz, *P*-O) ppm. IR (neat): $\tilde{\nu}$ = 3090–2890, 2381, 2346, 1592, 1479, 1455, 1436, 1281, 1135, 1106, 1068, 1011, 977, 893, 868, 764, 741, 717, 693, 621, 612 cm^{-1}. MS (EI): *m*/*z* (%) = 590 (10) $[M – H]^+$, 586 (30), 576 (100), 458 (10), 416 (30), 390 (20), 344 (30), 332 (40), 282 (45), 256 (50), 242 (95), 228 (50), 199 (50), 181 (100), 141 (80), 91 (55), 77 (45). $C_{35}H_{41}B_2NO_2P_2$ (591.238): C 71.10, H 6.99, N 2.37; found: C 71.04, H 7.14, N 2.51.

Compound 7p: 1.41 g (65%); white crystals (CH_2Cl_2/hexane); m.p. 210 °C. $[\alpha]_D^{20}$ = –52.4 (c = 1.5, $CHCl_3$); R_f = 0.25 (toluene). ^1H NMR ($CDCl_3$): δ = 0.30–1.80 (br, 6 H, BH_3), 1.36 (d, $^3J_{HH}$ = 6.5 Hz, 3 H, CH_3), 2.39 (d, $^3J_{PNCH}$ = 7.9 Hz, 3 H, NCH_3), 3.49 (s, 3 H, OCH_3), 3.54 (s, 3 H, OCH_3), 4.63 (m, 1 H, C*H*N), 5.43 (t, J = 9.3 Hz, 1 H, C*H*O), 6.62 (m, 2 H, *H* arom.), 6.84 (m, 2 H, *H* arom.), 6.95–7.15 (m, 9 H, *H* arom.), 7.20 (d, J_{HP} = 5.7 Hz, 2 H, *H* arom.), 7.28–7.40 (m, 4 H, *H* arom.), 7.45 (m, 2 H, *H* arom.), 7.60 (m, 1 H, *H* arom.), 7.90 (m, 1 H, *H* arom.) ppm. ^{13}C NMR ($CDCl_3$): δ = 15.7 (*C*H_3), 29.9 (d, $^2J_{PNC}$ = 4.7 Hz, N*C*H_3), 55.0 (O*C*H_3), 55.5 (O*C*H_3), 57.8 (dd, $^3J_{POCC}$ = 11.4, $^2J_{PNC}$ = 8.5 Hz, N*C*H), 82.7 (dd, $^3J_{PNCC}$ = 9.0, J_{POC} = 3.0 Hz, O*C*H), 111.6 (d, J_{PC} = 4.3 Hz, *C* arom.), 111.9 (d, J_{PC} = 5.3 Hz, *C* arom.), 118.7 (d, J_{PC} = 51.0 Hz, *C* arom.), 120.3 (d, J_{PC} = 70.9 Hz, *C* arom.), 120.9 (t, J_{PC} = 10.0 Hz, *C* arom.) 127.4–128.9 (*C* arom.), 129.6 (*C* arom.), 130.1 (d, J_{PC} = 10.6 Hz, *C* arom.), 130.7 (*C* arom.), 131.1 (d, J_{PC} = 12.0 Hz, *C* arom.), 131.9 (d, J_{PC} = 70.2 Hz, *C* arom.), 132.8 (d, J_{PC} = 57.5 Hz, *C* arom.), 133.2–134.0 (*C* arom.), 135.6 (d, J_{PC} = 12.2 Hz, *C* arom.), 138.5 (*C* arom.), 160.9 (d, J_{PC} = 4.4 Hz, *C* arom.) 161.0 (*C* arom.) ppm. ^{31}P NMR ($CDCl_3$): δ = 69.9 (br, *P*-N), 105.8 (br, *P*-O) ppm. IR (neat): $\tilde{\nu}$ = 3061–2896, 2383, 2349, 1590, 1573, 1477, 1458, 1431, 1278, 1252, 1220, 1163, 1134, 1064, 1008, 991, 959, 888, 868, 802, 758, 744, 712, 698, 614 cm^{-1}. MS (EI): *m*/*z* (%) = 620 (10) $[M^+$ -H], 620 (10), 606 (100) $[M^+ – H – BH_3]$, 589 (45), 573 (20), 561 (20), 545 (50), 500 (25), 485 (15), 471 (45), 453 (40), 438 (45), 390 (50), 374 (65), 363 (60), 317 (60), 286 (65), 272 (100), 256 (65), 245 (70), 228 (100), 215 (90), 199 (80), 183 (90), 170 (95), 151 (90), 137 (70), 123 (80), 107 (85), 91 (95), 77 (80). $C_{36}H_{43}B_2NO_3P_2$ (621.308): C 69.59, H 6.98, N 2.25; found: C 69.57, H 7.09, N 2.48.

General Procedure for Decomplexation into Free AMPP 4: The AMPP borane **7** (1 mmol) was placed in a three-necked flask fitted with a reflux condenser, a magnetic stirrer, and an argon inlet. A solution of DABCO (4 mmol) in toluene (6 mL) was added, and the flask was purged with three cycles of argon. The mixture was heated at 50 °C for 12 h and the crude product was rapidly filtered off on a neutral alumina column (15 cm height, 2 cm diameter) with use of toluene/AcOEt (9:1) as degassed eluent. After removal of the solvent, the free AMPP **4** was obtained in excellent yields and used without further purification.

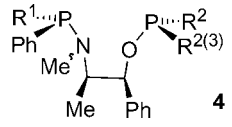

4

(*R*p)-{[(1*R*,2*S*)-2-(Diphenylphosphinito)-1-methyl-2-phenylethyl]-(methyl)amino}{*o*-[(2-methoxyethoxy)methoxy]phenyl}phosphane (4c): 560 mg (88%); white solid. ^1H NMR ($CDCl_3$): δ = 1.43 (d, $^3J_{HH}$ = 6.6 Hz, 3 H, CH_3), 2.17 (d, $^3J_{PNCH}$ = 2.7 Hz, 3 H, NCH_3), 3.24 (s, 3 H, OCH_3), 3.27–3.39 (m, 4 H, CH_2), 3.90 (m, 1 H, C*H*N), 4.76 (t, J = 8.9 Hz, 1 H, C*H*O), 4.97 (dd, J = 7.0, J = 26.7 Hz, 2 H, CH_2O), 6.56 (t, J = 7.1 Hz, 2 H, *H* arom.), 6.84 (t, J = 7.3 Hz, 1 H, *H* arom.), 6.92–7.48 (m, 22 H, *H* arom.) ppm. ^{31}P NMR ($CDCl_3$): δ = 55.1 (*P*-N), 111.7 (*P*-O) ppm.

Compound 4e: 634 mg (99%); orange crystals. ^1H NMR ($CDCl_3$): δ = 1.48 (d, $^3J_{HH}$ = 6.6 Hz, 3 H, CH_3), 2.14 (d, $^3J_{PNCH}$ = 3.0 Hz, 3 H, NCH_3), 3.91–4.20 (m, 2 H), 4.27 (s, 5 H, Cp), 4.32–4.35 (m, 2 H, Cp), 4.38–4.41 (m, 1 H, Cp), 4.79 (t, J = 8.7 Hz, 1 H, C*H*O), 6.85–6.90 (m, 2 H, *H* arom.), 7.08–7.43 (m, 16 H, *H* arom.), 7.57–7.64 (m, 2 H, *H* arom.) ppm. ^{31}P NMR ($CDCl_3$): δ = 62.3 (P-N), 111.6 (P–O) ppm.

Compound 4g: 590 mg (97%); white powder. ^1H NMR ($CDCl_3$): δ = 1.31 (d, $^3J_{HH}$ = 6.6 Hz, 3 H CH_3), 2.29 (d, $^3J_{PNCH}$ = 2.9 Hz, 3 H, NCH_3), 3.74 (m, 1 H, C*H*N), 4.86 (t, J = 8.5 Hz, 1 H, C*H*O), 6.68–6.71 (m, 2 H, *H* arom.), 7.04–7.06 (m, 2 H, *H* arom.), 7.10–7.18 (m, 1 H, *H* arom.), 7.20–7.35 (m, 18 H, *H* arom.), 7.40–7.50 (m, 4 H, *H* arom.), 7.57–7.62 (m, 2 H, *H* arom.) ppm. ^{31}P NMR ($CDCl_3$): δ = 57.3 (s, *P*-N), 111.95 (s, *P*-O) ppm.

Compound 4j: 523 mg (97%); white powder. ^{1}H NMR ($CDCl_3$): δ = 1.10–1.25 (m, 3 H), 1.35 (d, $^3J_{HH}$ = 6.7 Hz, 3 H, CH_3), 1.60–2.15 (m, 7 H), 2.35 (d, $^3J_{PNCH}$ = 3.2 Hz, 3 H, NCH_3), 3.84–3.89 (m, 1 H, C*H*N), 4.75 (t, *J* = 8.4 Hz, 1 H, C*H*O), 6.96–7.00 (m, 2 H, *H* arom.), 7.12–7.32 (m, 16 H, *H* arom.), 7.35–7.37 (m, 3 H, *H* arom.), 7.50–7.53 (m, 2 H, *H* arom.) ppm. ^{31}P NMR ($CDCl_3$): δ = 70.2 (*P*-N), 111.3 (*P*-O) ppm.

Compound 4l: 535 mg (90%). ^{1}H NMR ($CDCl_3$): δ = 1.46 (d, $^3J_{HH}$ = 6.7 Hz, 3 H, CH_3), 2.24 (d, $^3J_{PNCH}$ = 2.29 Hz, 3 H, NCH_3), 3.71 (s, 3 H, OCH_3), 3.97 (m, 1 H, C*H*N), 5.51 (t, *J* = 9.0 Hz, 1 H, C*H*O), 6.65–7.45 (m, 24 H, *H* arom.) ppm. ^{31}P NMR ($CDCl_3$): δ = 56.5 (P-*N*), 134.5 (P-*O*). The presence of a minor impurity was detected at 52.8 ppm.

Compound 4n: 529 mg (99%); white powder. ^{1}H NMR ($CDCl_3$): δ = 1.45 (d, $^3J_{HH}$ = 6.6 Hz, 3 H, CH_3), 2.24 (d, $^3J_{PNC}$ = 3.1 Hz, 3 H, NCH_3), 3.71 (s, 3 H, OCH_3), 4.00 (m, 1 H, C*H*N), 4.90 (t, *J* = 9.0 Hz, 1 H, C*H*O), 6.60–7.75 (m, 24 H, *H* arom.) ppm. ^{31}P NMR ($CDCl_3$): δ = 66.14 (s, *P*-N), 102.63 (s, *P*-O) ppm.

Compound 4o: 557 mg (99%); white powder. ^{1}H NMR ($CDCl_3$): δ = 1.30 (d, $^2J_{HP}$ = 6.6 Hz, 3 H, CH_3), 2.20 (d, $^3J_{HP}$ = 3.2 Hz, 3 H, NCH_3), 3.56 (s, 3 H, OCH_3), 4.00 (m, 1 H, C*H*N), 4.81 (t, *J* = 9.1 Hz, 1 H, C*H*O), 6.68–6.70 (m, 3 H, *H* arom.), 6.89 (t, 1 H, J_{HP} = 7.4, *H* arom.), 7.05–7.45 (m, 18 H, *H* arom.), 7.55–7.65 (m, 2 H, *H* arom.) ppm. ^{31}P NMR ($CDCl_3$): δ = 66.44 (s, *P*-N), 103.25 (s, *P*-O) ppm.

Compound 4p: 587 mg (99%); white powder. ^{1}H NMR ($CDCl_3$): δ = 1.55 (d, $^3J_{HH}$ = 6.6 Hz, 3 H, CH_3), 2.24 (d, $^3J_{PNCH}$ = 2.8 Hz, 3 H, NCH_3), 3.68 (s, 3 H, OCH_3), 3.71 (s, 3 H, OCH_3), 4.04 (m, 1 H, C*H*N), 4.87 (t, *J* = 8.6 Hz, 1 H, C*H*O), 6.55–7.80 (m, 23 H, *H* arom.) ppm. ^{31}P NMR ($CDCl_3$): δ = 56.77 (s, *P*-N), 102.37 (s, *P*-O) ppm.

Preparation of the Precatalyst AMPP-Rh Complexes. General Procedure: In a Schlenk tube, a solution of AMPP (0.020 mmol) in dry and degassed CH_2Cl_2 (1 mL) was added under argon at room temperature to $Rh(COD)_2BF_4$ (0.197 mmol) in dry and degassed CH_2Cl_2 (1 mL). The mixture was stirred for 1 h at room temperature. The CH_2Cl_2 was evaporated under vacuum to a volume of 0.5 mL and dry ether (5 mL) was added to precipitate the cationic complex. The precipitate was used for the asymmetric hydrogenation without further purification. In the case of the complex **9**, it was obtained as brown crystals by recrystallization from a CH_2Cl_2/hexane mixture.

Typical Procedure for the Hydrogenation of Methyl α-Acetamidocinnamate (1): Methyl α-Acetamidocinnamate (130 mg, 0.593 mmol), catalyst (prepared by the procedure described above, 3 mol%, 0.0197 mmol) and degassed dry solvent (8 mL) were introduced un-

Table 4. Crystallographic data for **7j** and **9**.

Compound	**7j**	**9**
Formula	$C_{34}H_{45}B_2NOP_2$	$C_{43}H_{47}NO_2P_2Rh$, BF_4
M	567.27	861.48
Crystallization	colorless crystal, from CH_2Cl_2/hexane	brown crystal, from CH_2Cl_2/hexane
Crystal system	triclinic	triclinic
Crystal size [mm]	0.28 × 0.20 × 0.10	0.22 × 0.2 × 0.15
Space group	*P*1	*P*1
a [Å]	9.9240(1)	10.7679(1)
b [Å]	12.6034(2)	11.2809(2)
c [Å]	15.0250(2)	19.0990(3)
α [°]	68.793(1)	96.842(1)
β [°]	81.887(1)	95.705(1)
γ [°]	71.235(1)	118.467(1)
V [Å^3]	1658.23(4)	1992.27(5)
Z	2	2
F (000)	608	888
$D_{calcd.}$ [g cm^{-3}]	1.136	1.436
Scan type	mixture of Φ rotations and ω scans	
μ [mm^{-1}]	0.157	0.565
$\sin(\theta)/\lambda_{max}$ [Å^{-1}]	0.65	0.65
Index ranges *h*/*k*/*l*	–12;12/–16;16/–19;19	–13;13/–14;14/–24;24
Absorption correction	Scalepack	
Reflections collected (RC)	14321	16811
Independent RC (IRC)	14321	16811
IRCGT = IRC and [$I > 2\sigma(I)$]	12348	15239
Refinement method	full-matrix, least-squares on F^2	
Data/restraints/parameters	14321/3/738	16811/3/978
R for IRCGT	R_1[a] = 0.0408, wR_2[b] = 0.0864	R_1[a] = 0.0399, wR_2[c] = 0.0798
R for IRC	R_1[a] = 0.053, wR_2[b] = 0.0919	R_1[a] = 0.0479, wR_2[c] = 0.0834
Goodness-of-fit[d]	1.025	1.032
Absol. structure parameter	0.03(4)	0.000(15)
Largest diff. peak and hole; e Å^{-3}	0.279 and –0.271	1.045 and –0.555

[a] $R_1 = \Sigma(||F_o| - |F_c||)/\Sigma|F_o|$. [b] $wR_2 = [\Sigma w(F_o^2 - F_c^2)^2/\Sigma[w(F_o^2)^2]^{1/2}$ where $w = 1/[\sigma^2(F_o^2) + 0.22P + (0.04P)^2]$ where $P = (\max(F_o^2, 0) + 2F_c^2)/3$. [c] $wR_2 = [\Sigma w(F_o^2 - F_c^2)^2/\Sigma[w(F_o^2)^2]^{1/2}$ where $w = 1/[\sigma^2(F_o^2) + 2.38P + (0.0171P)^2]$ where $P = (\max(F_o^2, 0) + 2F_c^2)/3$. [d] $[\Sigma w(F_o^2 - F_c^2)^2/(N_o - N_v)]^{1/2}$.

der argon into a 100 mL autoclave. Subsequently, the reactor was connected to a hydrogen cylinder. The argon was replaced with hydrogen by six pressurizing cycles and the hydrogenation was run under the reaction conditions indicated in the text. The solvent was removed under reduced pressure. The phenylalanine methyl ester **2** was purified by flash chromatography on silica gel with a toluene/AcOEt (3:1) mixture as eluent.

Phenylalanine Methyl Ester (2): ^{1}H NMR ($CDCl_3$): δ = 1.90 (s, 3 H, $COCH_3$), 3.04 (m, 2 H, CH_2Ph), 3.64 (s, 3 H, $COOCH_3$), 4.81 (m, 1 H, $CHCO_2CH_3$), 5.90 (br, 1 H, $NHCOCH_3$), 6.90–7.3 (m, 5 H, *H* arom.) ppm. ^{13}C NMR ($CDCl_3$): δ = 22.9 (s, $COCH_3$), 37.7 (s, CO_2CH_3), 52.1 (s, CH_2Ph), 53.1 (s, $CHCOOCH_3$), 127 (s, *C* arom.), 128.4 (s, *C* arom.), 129.1 (s, *C* arom.), 135.8 (s, *C* arom.), 169.6 (s, *C*O), 172.0 (s, *C*O) ppm.

X-ray Crystallographic Study of Complexes 7j and 9: The X-ray crystallographic analysis were collected with a Nonius Kappa CCD diffractometer at 110 K, with use of graphite-monochromated Mo-K_α radiation. The structure was solved by direct method (SHELXS-97)[67] and refined by full-matrix, least-squares methods (SHELXL-97)[67] with the aid of the WINGX program.[68] Crystallographic data are reported in Table 4.

CCDC-619377 and -619378 contain the supplementary crystallographic data for this paper. These data can be obtained free of charge from The Cambridge Crystallographic Data Centre via www.ccdc.cam.ac.uk/data_request/cif.

Acknowledgments

This work was supported by the Ministry of research, France, the CNRS, and Burgundy regional council. We would also like to thank Messrs. N. Morin (ENS Paris), N. Sellier (ENSCP Paris), B. Rebière, and E. Pousson (LSEO, Dijon) for the analysis and J. Rey for his help in synthesis.

[1] *Comprehensive Asymmetric Catalysis* (Eds: E. N. Jacobsen, A. Pfaltz, H. Yamamoto), Springer, New York, **2004**.
[2] R. Noyori, T. Ohkuma, *Angew. Chem. Int. Ed.* **2001**, *40*, 40–73.
[3] H. U. Blaser, C. Malan, B. Pugin, F. Spindler, H. Steiner, M. Studer, *Adv. Synth. Catal.* **2003**, *345*, 103–151.
[4] O. Riant, N. Mostefaï, J. Courmarcel, *Synthesis* **2004**, *18*, 2943–2958.
[5] X. Cui, K. Burgess, *Chem. Rev.* **2005**, *105*, 3272–3296.
[6] C. Jäkel, R. Paciello, *Chem. Rev.* **2006**, *106*, 2912–2942.
[7] L. F. Tietze, I. Hiriyakkanavar, H. P. Bell, *Chem. Rev.* **2004**, *104*, 3453–3516.
[8] H. M. L. Davies, R. E. J. Beckwith, *Chem. Rev.* **2003**, *103*, 2861–2903.
[9] B. M. Trost, M. L. Crawley, *Chem. Rev.* **2003**, *103*, 2921–2923.
[10] M. Shibasaki, E. M. Vogl, T. Ohshima, *Adv. Synth. Catal.* **2004**, *346*, 1533–1552.
[11] A. M. Carroll, T. P. O'Sullivan, P. J. Guiry, *Adv. Synth. Catal.* **2005**, *347*, 609–631.
[12] H. Ibrahim, A. Togni, *Chem. Commun.* **2004**, 1147–1155.
[13] K. B. Sharpless, *Angew. Chem. Int. Ed.* **2002**, *41*, 2024–2032.
[14] E. N. Jacobsen, M. H. Wu in *Comprehensive Asymmetric Catalysis*, vol. II (Eds: E. N. Jacobsen, A. Pfaltz, H. Yamamoto), Springer, Heidelberg, **1999**, chapter 21, pp. 649–677.
[15] H. C. Kolb, K. B. Sharpless, *Asymmetric dihydroxylation* in *Transition Metals for Organic Synthesis*, 2nd ed., vol. 2 (Eds.: M. Beller, C. Bolm), Wiley-VCH, Weinheim, Germany, **2004**, pp. 275–298.
[16] W. Tang, X. Zang, *Chem. Rev.* **2003**, *103*, 3029–3069.
[17] M. Berthod, G. Migniani, G. Woodward, M. Lemaire, *Chem. Rev.* **2005**, *105*, 1801–1836.
[18] T. P. Clark, C. R. Landis, *Tetrahedron: Asymmetry* **2004**, *15*, 2123–2137.
[19] H. A. McManus, P. J. Guiry, *Chem. Rev.* **2004**, *104*, 4151–4202.
[20] M. van den Berg, A. J. Minnaard, E. P. Schudde, J. van Esch, A. H. M. de Vries, J. G. de Vries, B. L. Feringa, *J. Am. Chem. Soc.* **2000**, *122*, 11539–11540.
[21] M. Dieguez, O. Pamies, C. Claver, *Chem. Rev.* **2004**, *104*, 3189–3215.
[22] M. Tanaka, I. Ogata, *J. Chem. Soc., Chem. Commun.* **1975**, 735.
[23] R. H. Grubbs, R. A. deVries, *Tetrahedron Lett.* **1977**, *22*, 1879–1880.
[24] M. T. Reetz, T. Sell, *Tetrahedron Lett.* **2000**, *41*, 6333–6336.
[25] M. van den Berg, A. J. Minnaard, R. M. Haak, M. Leeman, E. P. Schudde, A. Meetsma, B. L. Feringa, A. H. M. de Vries, C. E. P. Maljaars, C. E. Willans, D. Hyett, J. A. F. Boogers, H. J. W. Henderickx, J. G. de Vries, *Adv. Synth. Catal.* **2003**, *345*, 308–323.
[26] H. J. Kreuzfeld, U. Schmidt, C. Döbler, H. W. Krause, *Tetrahedron: Asymmetry* **1996**, *7*, 1011–1018.
[27] F. Agbossou, J. F. Carpentier, F. Hapiot, I. Suisse, A. Mortreux, *Coord. Chem. Rev.* **1998**, *178–180*, 1615–1645.
[28] E. A. Broger, W. Burkart, M. Hennig, M. Scalone, R. Schmidt, *Tetrahedron: Asymmetry* **1998**, *9*, 4043–4054.
[29] O. Lot, I. Suisse, A. Mortreux, F. Agbossou, *J. Mol. Catal. A* **2000**, *164*, 125–130.
[30] G. Chen, X. Li, H. Zhang, L. Gong, A. Mi, X. Cui, Y. Jiang, M. C. K. Choi, A. S. C. Chan, *Tetrahedron: Asymmetry* **2002**, *13*, 809–813.
[31] N. V. Dubrovina, V. I. Tararov, Z. Kadyrova, A. Monsees, A. Börner, *Synthesis* **2004**, *12*, 2047–2051.
[32] B. D. Vineyard, W. S. Knowles, M. J. Sabacky, G. L. Bachman, D. J. Weinkauff, *J. Am. Chem. Soc.* **1977**, *99*, 5946–5952.
[33] W. S. Knowles, *Acc. Chem. Res.* **1983**, *16*, 106–112.
[34] A. Marinetti, S. Jus, J. P. Genêt, *Tetrahedron Lett.* **1999**, *40*, 8365–8368.
[35] I. D. Gridnev, T. Imamoto, *Acc. Chem. Res.* **2004**, *37*, 633–644.
[36] J. M. Brown, P. A. Chaloner, *J. Am. Chem. Soc.* **1980**, *102*, 3040–3048.
[37] A. S. C. Chan, J. J. Pluth, J. Halpern, *J. Am. Chem. Soc.* **1980**, *102*, 5952–5954.
[38] A. S. C. Chan, J. Halpern, *J. Am. Chem. Soc.* **1980**, *102*, 838–840.
[39] P. S. Chua, N. K. Roberts, B. Bosnich, S. J. Okrasinski, J. Halpern, *J. Chem. Soc., Chem. Commun.* **1981**, *102*, 1278–1280.
[40] C. R. Landis, J. Halpern, *J. Am. Chem. Soc.* **1987**, *109*, 1746–1754.
[41] U. Nagel, B. Rieger, *Organometallics* **1989**, *8*, 1534–1538.
[42] J. S. Giovannetti, C. M. Kelly, C. R. Landis, *J. Am. Chem. Soc.* **1993**, *115*, 4040–4057.
[43] C. R. Landis, P. Hilfenhaus, S. Feldgus, *J. Am. Chem. Soc.* **1999**, *121*, 8741–8754.
[44] S. Feldgus, C. R. Landis, *J. Am. Chem. Soc.* **2000**, *122*, 12714–12727.
[45] R. Giernoth, H. Heinrich, N. J. Adams, R. J. Deeth, J. Bargon, J. M. Brown, *J. Am. Chem. Soc.* **2000**, *122*, 12381–12382.
[46] C. R. Landis, S. Feldgus, *Angew. Chem. Int. Ed.* **2000**, *39*, 2863–2866.
[47] I. D. Gridnev, N. Higashi, K. Asakura, T. Imamoto, *J. Am. Chem. Soc.* **2000**, *123*, 7183–7194.
[48] I. D. Gridnev, T. Imamoto, *Organometallics* **2001**, *20*, 545–549.
[49] H. Heinrich, R. Giernoth, J. Bargon, J. M. Brown, *Chem. Commun.* **2001**, 1296–1297.
[50] I. D. Gridnev, N. Higashi, T. Imamoto, *Organometallics* **2001**, *20*, 4542–4553.
[51] I. D. Gridnev, M. Yasutake, N. Higashi, T. Imamoto, *J. Am. Chem. Soc.* **2001**, *123*, 5268–5376.
[52] K. V. L. Crépy, T. Imamoto, *Adv. Synth. Catal.* **2003**, *345*, 79–101.

[53] Y. Wada, T. Imamoto, H. Tsuruta, K. Yamaguchi, I. D. Gridnev, *Adv. Synth. Catal.* **2004**, *346*, 777–788.
[54] T. Schmidt, W. Baumann, H.-J. Drexler, A. Arrieta, D. Heller, H. Buschmann, *Organometallics* **2005**, *24*, 3842–3848.
[55] G. Hoge, H.-P. Wu, W. S. Kissel, D. A. Pflum, D. J. Greene, J. Bao, *J. Am. Chem. Soc.* **2004**, *126*, 5966–5967.
[56] D. Moulin, C. Darcel, S. Jugé, *Tetrahedron: Asymmetry* **1999**, *10*, 4729–4743.
[57] For modified P-chirogenic EPHOS ligands **4′** derived from (–)-ephedrine with R^1 = Me, *n*-Bu, 1-Np and R^2 = R^3 = Ph, *p*-Tol, 3,5-$(CF_3)_2$Ph, see: R. Ewalds, E. B. Eggeling, A. C. Hewat, P. C. J. Kamer, P. W. N. M. van Leeuwen, D. Vogt, *Chem. Eur. J.* **2000**, *6*, 1496–1504 and Ref.[58].
[58] J. J. Carbo, A. Lledos, D. Vogt, C. Bo, *Chem. Eur. J.* **2006**, *12*, 1457–1467.
[59] E. B. Kaloun, R. Merdès, J. P. Genêt, J. Uziel, S. Jugé, *J. Organomet. Chem.* **1997**, *529*, 455–463.
[60] C. Bauduin, D. Moulin, E. B. Kaloun, C. Darcel, S. Jugé, *J. Org. Chem.* **2003**, *68*, 4293–4301.
[61] P. Haquette, F. Lebideau, S. Dagorne, J. Marrot, G. Jaouen, *Acta Crystallogr., Sect. C* **2002**, *58*, m551–m552.
[62] P-chirogenic AMPP ligands **4e** and **4g** were also investigated in asymmetric allylation catalyzed by palladium complexes: C. Darcel et al., manuscript in preparation.
[63] The computations were performed with PC-Model Version 7.0 from Serena Software (MMX and MM3 force field). For appropriate modeling of the hydrides, these were replaced by F atoms, which exhibit the same atomic radii and M–H bond lengths.
[64] H.-J. Drexler, S. Zhang, A. Sun, A. Spannenberg, A. Arrieta, A. Preetz, D. Heller, *Tetrahedron: Asymmetry* **2004**, *15*, 2139–2150.
[65] A. Kless, R. Kadyrov, A. Börner, J. Holz, H. B. Kagan, *Tetrahedron Lett.* **1995**, *36*, 4601–4602.
[66] The organolithium reagents are prepared by bromide metal exchange with *sec*-butyllithium as described previously.[56] In the case of the ferrocenyllithium, it was prepared by deprotonation of ferrocene with 1 equiv. of butyllithium in THF at –78 °C.
[67] G. M. Sheldrick, *SHELX97* (includes *SHELXS97* and *SHELXL97*), Release 97-2, Programs for Crystals Structure Analysis, University of Göttingen, Göttingen, Germany, **1998**.
[68] L. J. Farrugia, *J. Appl. Crystallogr.* **1999**, *32*, 837–838.

Received: November 5, 2006
Published Online: March 14, 2007

